Journal of Biomechanics 185 (2025) 112687

Contents lists available at ScienceDirect

Journal of Biomechanics

journal homepage: www.elsevier.com/locate/jbiomech

Is IMU- alternative to GRF-based posturography? A comparative assessment on young healthy adults

Maria Cristina Bisi *, Rita Stagni

Department of Electrical, Electronic and Information Engineering "Guglielmo Marconi", University of Bologna, Via del Risorgimento 2, 40136 Bologna, Italy
Interdepartmental Center for Industrial Research On Health Sciences & Technologies, University of Bologna, Bologna 40064, Italy

ARTICLE INFO

Keywords:
Posturography
Inertial sensors
Postural control

ABSTRACT

The measurement of CoP trajectory has become the de-facto standard for posturography. However, in recent years, inertial sensors have been proposed as a portable alternative to force plates. Although their demonstrated potential, the functional interpretation of these methods remains limited, and no standard approach exists for inertial signal processing.

This work aims to analyse and compare GRF- and IMU-based metrics (obtained from a single IMU positioned on the trunk at L5 level) in characterising postural control performance in 21 healthy participants on varying surface (i.e. solid ground and three foams of different stiffness) and visual (eyes open/closed) conditions, concurrently analysing how results are affected by different filtering cut-off frequencies.

In line with existing literature, GRF signals were lowpass-filtered at 10 Hz, while IMU signals at 0.5 Hz, 3.5 Hz, 5 Hz (i.e. band-width containing 95 % of the signal power), and 10 Hz. Time- and frequency-domain postural parameters were extracted from GRF and IMU signals.

Correlations between GRF- and IMU-based metrics resulted weak to moderate ($0<|\rho|<0.7$). Both GRF- and IMU-based metrics showed increased postural oscillations on foam surfaces, but opposite behaviours in frequency, with no significant difference among different foam types. GRF-based metrics highlighted higher postural oscillations under eyes-closed conditions, especially on foam, whereas IMU-based metrics showed no significant change except for range and root mean square displacement in the medio-lateral direction that decreased with eyes closed (e.g., 5 Hz low pass filtered IMU signal: on foam, median root mean square, with eyes open [25th-75th], 0.08 [0.05–0.12]; with eyes closed, 0.04 [0.03–0.06]).

Although describing the same behaviour, GRF- and IMU-based metrics capture different aspects of postural control: based on the inverted pendulum model, GRF-based metrics describe the postural adjustments, while IMU-based ones the postural performance.

1. Introduction

Postural control is defined as the ability to sustain, achieve, or regain balance during any posture or activity (Pirini et al., 2018). Effective postural control is essential for performing daily activities, necessitating the integration of information processed by the somatosensory, visual, and vestibular systems to maintain a stable, upright posture with adaptive orientation and balance strategies (Pirini et al., 2018). This integration requires a complex interaction between sensory and motor systems to manage the body's multi-segmental structure and limb coordination. Consequently, conditions that disrupt or alter proprioception, vision, and/or vestibular functions (e.g., neuropathy, visual impairments, and inner ear disorders) can significantly impair postural control performance (i.e. postural sway). Experimentally, methods aiming to reproduce these altered conditions are often used to test postural control, allowing the investigation of sensory integration in healthy and pathological subjects (Paillard and Noé, 2015). In such tests, postural sway performs better when subjects have access to multiple accurate sensory sources for orientation (e.g., standing on a flat, level surface with eyes open), as all sensory systems provide consistent information. When the eyes are closed or while standing on a compliant foam surface, visual and proprioceptive cues are respectively removed or distorted, leading to increased sway, highlighting the role of vision and proprioception in maintaining balance (Peterka, 2018).

* Corresponding author.
E-mail addresses: mariacristina.bisi@unibo.it (M.C. Bisi), rita.stagni@unibo.it (R. Stagni).

https://doi.org/10.1016/j.jbiomech.2025.112687
Accepted 8 April 2025
Available online 9 April 2025

The standard method for postural sway assessment is to measure and record the trajectory of the centre of pressure (CoP) using a force plate during quiet standing. This approach is based on the assumption that the trajectory of the CoP (i.e., the point of application of the resultant ground reaction force (GRF)) is the result of the dynamic neuromuscular response to control the position of the body's centre of mass (CoM).

Based on this assumption, various GRF-based metrics have been proposed to characterize the mechanisms involved in postural regulation (Paillard and Noé, 2015), calculated either on the statokinesigram (CoP trajectory map in the horizontal plane) or on the stabilogram (time series variations of the CoP in the antero-posterior (AP) and medio-lateral (ML) directions) in both the time and frequency domains.

Time-domain variables characterize the magnitude of the resultant and/or the ML and AP components of the CoP trajectory. Typically, greater magnitudes or deviations of these variables are associated with poorer postural stability (Paillard and Noé, 2015). Frequency-domain parameters (e.g., mean, median, centroid, and 80–95 % power frequency) provide an overall representation of the CoP signal's frequency content. Higher postural sway frequencies are interpreted as postural control determining faster and smaller postural adjustments (Paillard and Noé, 2015). Total power frequency is considered an index of energy expenditure, and changes in the distribution of frequency bands may reflect modifications in the preferential involvement of specific neuronal loops in postural regulation (Paillard and Noé, 2015).

These variables have been found to be sensitive in differentiating young and old individuals, as well as healthy subjects from neurologically impaired patients, allowing for the quantification and analysis of postural deficits (Paillard and Noé, 2015). However, the portability of force platforms is limited and not suitable to any ambulatory condition (Mancini et al., 2012), therefore, inertial measurement units (IMUs) have been proposed as a truly portable, low-cost alternative to force platforms for studying postural control (Ghislieri et al., 2019; Mancini et al., 2012).

IMU-based posturography utilizes acceleration data (ACC) from sensors attached to the body, the most common sensor location being on the back at L5 level, assuming that it approximates of the centre of mass (CoM) acceleration (CoM-ACC) during standing (Ghislieri et al., 2019). Various frequency- and time-domain metrics are then directly extracted from the collected ACC signal: most IMU-based metrics proposed in the literature are derived from GRF-based ones and are applied, with the same mathematical formulation, on ACC signals (Ghislieri et al., 2019; Mancini et al., 2012; Palmerini et al., 2011), despite being conceptually different signals. For example, time-domain postural parameters have spatial properties because the CoP represents a displacement, yet they are applied directly to trunk ACC (approximating CoM-ACC), even though it conveys different information (Ghislieri et al., 2019).

Understanding how CoP trajectory relates to CoM-ACC, thus, how GRF-based metrics relate to IMU-based ones, is essential for the functional interpretation of the results of both approaches. Based on the inverted pendulum model of quiet standing (Winter, 1995) (see Fig. 1), CoM-ACC in the horizontal plane is proportional to the difference between CoP and CoM position (Gage et al., 2004; Winter, 1995). Therefore, GRF- and IMU-based metrics may have a similar mathematical formulation, but, being applied to CoP trajectory and to (an approximation of) CoM-ACC, respectively, they quantify different aspects of posture, hindering direct comparison between the two methods (Noamani et al., 2023). According to the literature (Ghislieri et al., 2019), as long as IMUs allow to quantify relevant information to characterize postural balance, the lack of direct comparability with traditional GRF-based metrics can be considered inconsequential (Ghislieri et al., 2019; Mancini et al., 2012).

Winter suggested that CoM-ACC might be even a more effective measure of postural sway, as it represents the error signal within the postural control system (Noamani et al., 2023; Winter, 1995). However, to date, IMU-based posturography has primarily been used to differentiate populations (e.g. young vs elderly adults, healthy vs parkinsonians, parkinsonians on vs off therapy), rather than to develop hypotheses for the functional interpretation of the resulting metrics (Ghislieri et al., 2019).

Before attempting to provide a physiological interpretation of IMU-based posturographic metrics, literature review highlights several gaps and topics that need to be addressed by future research (Ghislieri et al., 2019; Noamani et al., 2023). In particular, comparative sensitivity of GRF- and IMU-based metrics to testing conditions and processing must

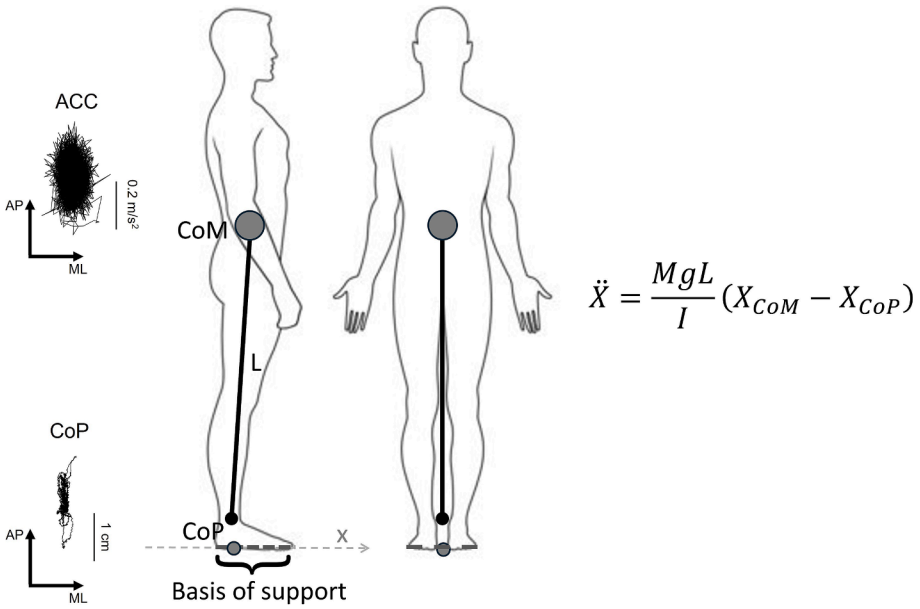

Fig. 1. On the right, schematic representation of the simplified inverse pendulum model for quite standing posture and corresponding differential equation for dynamics control: CoM is the centre of mass (of the whole body of mass M, approximating that of the body minus the feet); CoP is the centre of pressure (point of application of the resultant ground reaction force); L is the length of the pendulum corresponding to the distance between the centre of the ankle and the CoM); *g* is the gravitational acceleration; I is the moment of inertia of the body (minus the feet) with respect to the centre of the ankles. On the left, exemplificative ACC and CoP statokinesigrams.

Table 1
The dimensions, density and elastic modulus of the foam blocks used in this study.

Foam material	Dimensions, length × width × height (cm)	Density (kg/m3)	Elastic modulus (kPa)	1st derivative of the stress–strain curve in the densification region (kPa)
Soft (SF)	30 × 53 × 10	28.6	32.8	465
Medium (MF)	30 × 53 × 10	24.8	51.9	347
Firm (FF)	30 × 53 × 10	25.1	139.2	344

be assessed, and acquisition and processing protocols require standardisation.

Regarding protocols, there is no consensus on the filtering of ACC signal, most postural oscillations occur at low frequencies, but different upper bandwidth limits have been used in IMU-based studies, ranging from 0.5 Hz to no filtering (Dalton et al., 2013; Ghislieri et al., 2019). Palmerini et al. (Palmerini et al., 2011) suggested using a 0.5 Hz low-pass filter to estimate CoM displacement from trunk acceleration data. Other studies have employed a 3.5 Hz or 3 Hz cut-off frequency, initially proposed to remove tremor-related accelerations in Parkinson's patients, but subsequently applied to other populations (Gera et al., 2018; Huisinga et al., 2018; Mancini et al., 2012). In the literature, some studies used higher cut-off frequencies: in particular one used 30 Hz, based on the observation that more than 95 % of the signal power was below 15 Hz in adults (Reynard et al., 2019) and one analysed raw acceleration signal to ensure that no information was lost or altered (Dalton et al., 2013). However, it is important to note that both of these studies examined, with the same filtering procedure, not only motor performance during quiet standing but also during other tasks, such as standing on one leg or a rocking board (Reynard et al., 2019) and gait (Dalton et al., 2013). Clearly, as filtering methods may influence results (Miller et al., 2022), further investigation is required.

In addition, to verify how IMU-based metrics perform with respect to the standard GRF-based ones and to better understand their functional interpretation, it is necessary to assess their potential to detect mild changes in postural control performance in response to different operative conditions of the same population. Thus, the aim of the present work was to compare IMU- and GRF-based posture metrics, in both time and frequency domain, in a population of young healthy adults for changing visual and surface conditions, concurrently analysing how results are affected by filtering of ACC signal.

2. Materials and methods

2.1. Study subjects

Twenty-one healthy adults (11 females / 10 males, age 24 ± 3 years, height 1.71 ± 0.1 m, body mass 64 ± 10 kg, BMI 24 ± 3 kg/m^2) participated in the study. All participants had no known musculoskeletal pathology, severe visual or hearing impairment. The Review Board Committee of the authors' institution approved this study, and informed consent was obtained from the participants.

2.2. Experimental protocol

The participants were assessed wearing comfortable clothes. The assessment took place in a well-lit and ventilated room with adequate heat and sound. Participants were instructed to stand on a force-platform (type 4060-08, Bertec, USA), barefoot, with their arms hanging at their sides and their feet positioned conformably under their hips. Each participant was allowed to externally rotate their feet to a comfortable extent (McIlroy and Maki, 1997). The self-selected distance between heels was measured and maintained across different conditions analysed. A tri-axial wireless inertial sensor (Miniwave, Cometa s.r.l., Italy) was positioned on the lower trunk at the L5 level using tape, with sensing axes oriented along the anatomical vertical (V-x), medio-lateral (ML-y), and antero-posterior (AP-z) directions.

3D IMU acceleration (286 Hz sampling frequency; 2 g full scale) and 3D GRF (800 Hz sampling frequency) signals were acquired for 60 s during quiet standing posture of each subject 8 times:

- over 4 surfaces: solid surface (no foam, NF) and three foam blocks of increasing stiffness (Patel et al., 2008) - soft foam (SF), medium foam (MF), firm foam (FF) (characteristics of the foams are reported in Table 1);
- with eyes open (EO) and with eyes closed (EC) on each surface.

A trigger signal generated by IMU system was registered at the beginning of each trial for synchronization.

The sequence of surface conditions was randomized to minimize potential order effects. To prevent fatigue, a 2-minute rest period was planned among tests. During the EO condition, participants were instructed to fix their gaze straight ahead on a cross-shaped target placed 2.5 m away at eye level.

Participants were asked which foam they found most task-demanding, without being provided any information about stiffness.

2.3. Data analysis

The first 10 s of each trial were discarded to avoid transients and 40 s of time recordings were analysed.

To enhance comparisons with the most used sampling frequency in literature (Ghislieri et al., 2019), all collected signals were resampled at 100 Hz after applying a 4th-order zero-lag Butterworth low-pass filter with a cut-off frequency of 50 Hz to prevent aliasing.

Thirteen GRF- and IMU-based postural metrics in the time and frequency domain were identified from literature review (Mancini et al., 2012). Table 2 provides a brief description of each metric (Mancini et al., 2012; Palmerini et al., 2011) and the direction along which they were computed (AP, ML, and/or 2D vector's magnitude, module). Further details on time domain metrics calculation are provided in the Appendix.

The CoP trajectory recorded by the force-plate was filtered using a 10 Hz cut-off, fourth-order, zero-phase, low-pass Butterworth filter (Quijoux et al., 2021).

The vertical component of trunk acceleration was neglected (Mancini et al., 2012; Palmerini et al., 2011), as postural sway occurs mainly in the transverse plane.

All time and frequency domain metrics were calculated from 10 Hz filtered CoP trajectory and raw acceleration components (ACC_raw in AP and ML directions) for each subject and each testing condition.

The maximum value of frequency containing 95 % of the power of ACC_raw (for all trials in both AP and ML directions, including all participants and all conditions) was calculated (f95max).

ACC_raw signal components in AP and ML directions were lowpass-filtered (using a fourth-order, zero-phase, low-pass Butterworth filter) at the following cut-off frequencies: 0.5 Hz (ACC_0.5), 3.5 Hz (ACC_3.5), f95max (ACC_f95), and 2*f95max (ACC_2f95).

Only time domain metrics were also calculated from ACC_0.5, ACC_3.5, ACC_f95, ACC_2f95 for each subject and each testing condition.

Table 2
Analysed postural metrics, in the columns are reported from left to right: acronym, domain, brief description (Mancini et al., 2012; Palmerini et al., 2011), direction along which they were computed (AP, ML, and 2D vector's magnitude, module).

Measure	Domain	Description	Directions
F50	frequency	50 % power frequency: frequency containing 50 % or the total power	module, AP, ML
F80	frequency	80 % power frequency: frequency containing 80 % or the total power	module, AP, ML
F95	frequency	95 % power frequency: frequency containing 95 % or the total power	module, AP, ML
PWR	frequency	Total power	module, AP, ML
CF	frequency	Centroidal frequency: the frequency at which spectral mass is concentrated	module, AP, ML
FD	frequency	Frequency dispersion	module, AP, ML
DIST	time	Mean distance from the center of signal trajectory	module, AP, ML
RMS	time	Root mean square of signal time series	module, AP, ML
PATH	time	Sway path, total length of signal trajectory	module, AP, ML
RANGE	time	Range of displacement	module, AP, ML
MV	time	Mean Velocity	module, AP, ML
MF	time	Mean frequency, the number, per second, of loops that have to be run by CoP/ACC, to cover a total trajectory equal to PATH (MF = PATH/(2*π*DIST*trial duration)	module
AREA	time	area spanned from the 2D signal vector per unit of time	module

2.4. Statistical analysis

A Kolmogorov–Smirnov test was performed to test normal distribution of the estimated parameters, and normal distribution was not verified.

Spearman's correlation coefficients, ρ, (significance level 0.05) were calculated comparing GRF- to IMU-based results for each metric. For frequency domain parameters only ACC_raw was considered; for time-domain parameters, GRF-based were compared to IMU-based results also for ACC_0.5, ACC_3.5, ACC_f95, ACC_2f95. Spearman's correlation coefficients were interpreted according to Schober et al. (Schober et al., 2018) using the following thresholds: no correlation ($|\rho| < 0.1$), weak correlation ($0.1 \leq |\rho| < 0.4$), moderate correlation ($0.4 \leq |\rho| < 0.7$), and strong correlation ($|\rho| \geq 0.7$).

A Scheirer–Ray–Hare test (significance level 0.05) was applied to test the effect of surface and visual condition on GRF- and IMU-based metrics. In absence of interaction between surface and visual conditions, the subsequent statistical analysis was performed separately *per* factor.

A Kruskal-Wallis test (significance level 0.05) was performed to test the effect of surface conditions on GRF- and IMU-based metrics, for EO and EC conditions, separately. When a significant effect was detected, a multiple comparison test (Hochberg and Tamhane, 2008) was used to determine which specific condition resulted significant. A Dunn–Sidak correction was applied for post-hoc analysis.

To test differences between EC and EO conditions, a Wilcoxon signed rank test for repeated measures was applied on the entire dataset and for the different surface conditions separately (significance level 0.05).

Data processing and statistical analyses were performed in MATLAB2023a (MathWorks BV, Natick, MA).

3. Results

3.1. Frequency content of CoP and ACC signals

F95 calculated on CoP trajectory ranged between 0.6 Hz and 2.1 Hz, F80 between 0.3 Hz and 1.4 Hz, and F50 between 0.2 Hz and 0.9 Hz. F95 calculated on ACC_raw ranged between 3.4 Hz and 4.9 Hz, F80 between 1.5 Hz and 4.2 Hz, and F50 between 0.5 Hz and 2.6 Hz. Since maximal F95 for IMU-signals resulted 4.9 Hz, f95max was approximated to 5 Hz.

Fig. 2 shows F95, F80, and F50 calculated on a) CoP trajectory and on b) ACC_raw in the different conditions. Detailed numerical values for each condition are shown in Table S1 (supplementary material).

3.2. GRF- and IMU-based metrics

Distribution of frequency and time-domain metrics (25th, 50th and 75th percentiles) obtained from the different analysed signals (i.e., CoP, ACC_raw, ACC_2f95, ACC_f95, ACC_3.5 and ACC_0.5) and for the different conditions (surface conditions: NF, SF, MF, FF; visual condition: EO, EC) are reported in the supplementary material (Table S1).

3.3. Correlation between GRF- and IMU-based metrics

In the frequency domain, only power parameters (PWR, PWR AP, and PWR ML) demonstrated moderate positive correlations between the ones calculated from CoP and the ones from ACC_raw ($\rho = 0.45$, 0.45, and 0.57, respectively) (Table 3). Other parameters showed either weak negative correlation (i.e., F50, F50 AP, F80, F80 AP, F95, F95 AP, F95 ML, CF, CF AP, FD, FD AP) either no correlation (F50 ML, F80 ML, CF ML, FD ML).

In the time domain, results showed significant positive correlations ($\rho > 0.1$) for most parameters calculated using CoP and all acceleration signals (i.e., DIST, DIST AP, DIST ML, RMS, RMS AP, RMS ML, RANGE, RANGE AP, RANGE ML, AREA), except for: MF for all acceleration signals; PATH, PATH AP, PATH ML, MV, MV AP, and MV ML for ACC_raw only. ACC_3.5 exhibited the highest number of moderate positive correlations ($\rho > 0.40$). The only parameters showing positive weak correlations were DIST AP, RMS AP, and RANGE AP. Table 3 presents the ρ values for each parameter, calculated from CoP and the differently filtered acceleration signals, considering all conditions together. 95 % confidence intervals and p-values for each correlation coefficient are provided.

3.4. Effect of surface condition

Refer to Table S1 for detailed numerical data.

3.4.1. Frequency domain parameters

Participants showed significantly increased GRF-based PWR, PWR

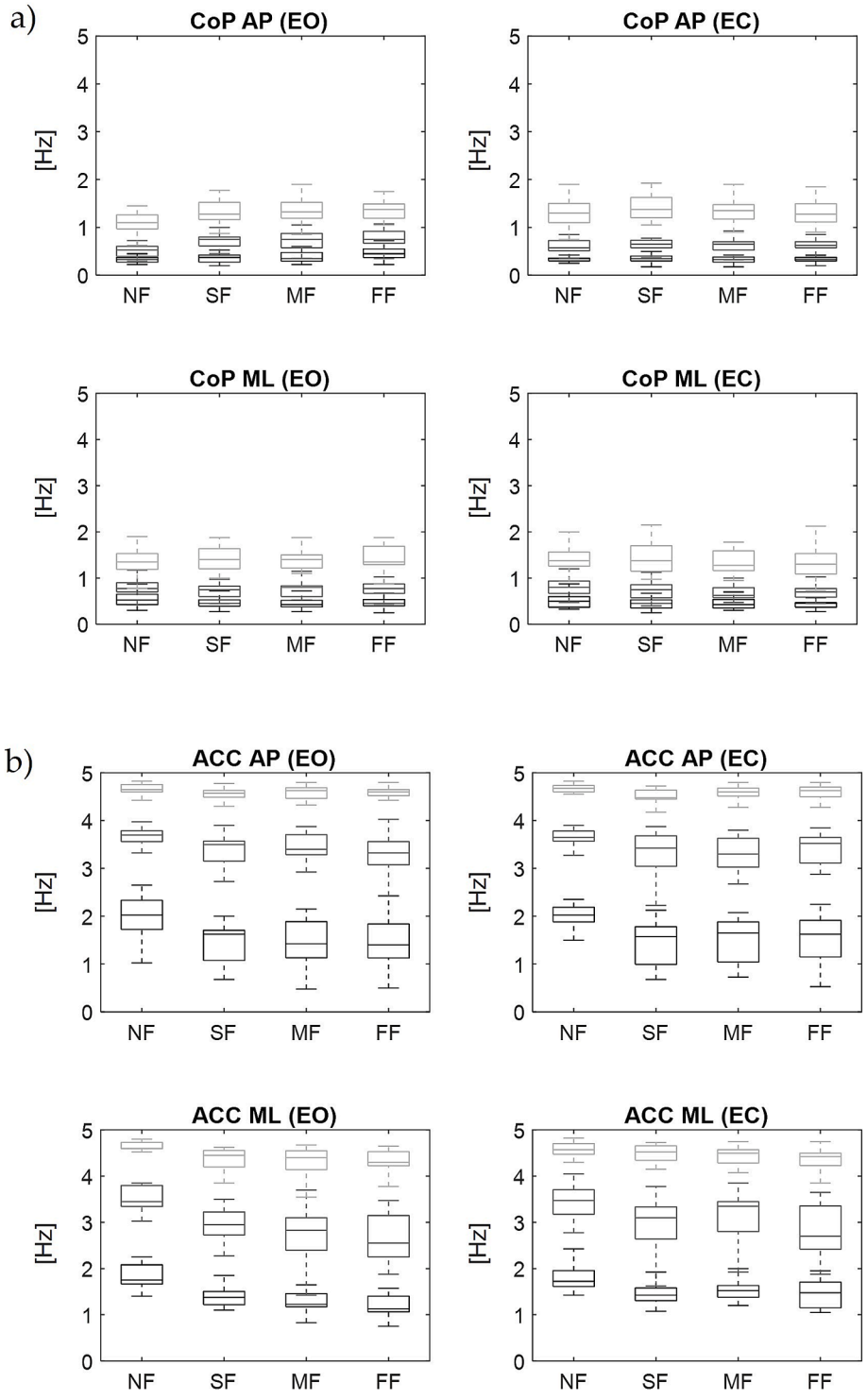

Fig. 2. F50 (black), F80 (dark grey), and F95 (light grey) of the anteroposterior (AP) and mediolateral (ML) components of a) CoP and b) ACC in the different conditions (no foam, NF, soft foam, SF, medium foam, MF, firm foam, FF, eyes open, EO, and eyes closed, EC).

AP, CF, and CF AP when standing on any foam. No other significant difference was observed for other metrics.

When considering ACC_raw, PWR and PWR AP increased, while F50 (F50, F50 AP, and F50 ML), and CF (CF, CF AP, and CF ML) decreased significantly on foam surfaces.

No difference was found with post-hoc analysis among the three foams.

3.4.2. Time domain parameters

All GRF-based time-domain metrics increased when standing on a foam, both with EO and EC, with the exception of MF that was not affected. Post-hoc analysis revealed no difference among foams.

Similar results were observed for all time-domain metrics from IMU-based signals (i.e., ACC_raw, ACC_2f95, ACC_f95, ACC_3.5, and ACC_0.5), with the exception of PATH and MV from ACC_raw or ACC_2f95 that did not show any effect of surface condition, and MF from ACC_raw that decreased when standing on a foam.

Table 3
Spearman's correlation coefficients (ρ) for each parameter: (a) frequency-domain and (b) time-domain, calculated on CoP and the differently filtered acceleration signals, considering all conditions together. For each correlation coefficient, the 95 % confidence interval is shown in brackets, and p-values are provided. Values are displayed only when $|\rho| > 0.1$. Moderate correlations are highlighted in bold.

a)

	ACC_raw	p-value
F50	-0.19 [-0.33:-0.04]	1.5E-02
F50 AP	-0.20 [-0.36:-0.06]	7.9E-03
F50 ML	–	–
F80	-0.23 [-0.37:-0.07]	2.9E-03
F80 AP	-0.19 [-0.33:-0.04]	1.5E-02
F80 ML	–	
F95	-0.25 [-0.39:-0.09]	8.9E-04
F95 AP	-0.29 [-0.43:-0.13]	1.3E-04
F95 ML	-0.16 [-0.30:-0.02]	3.4E-02
PWR	**0.45 [0.32:0.56]**	1.2E-09
PWR AP	**0.45 [0.34:0.58]**	6.6E-10
PWR ML	**0.57 [0.45:0.66]**	9.7E-16
CF	-0.25 [-0.41:-0.10]	9.4E-04
CF AP	-0.32 [-0.46:-0.18]	2.2E-05
CF ML	–	–
FD	-0.11 [-0.25:0.03]	1.4E-01
FD AP	-0.15 [-0.30:0.00]	5.6E-02

(*continued on next page*)

Table 3 (*continued*)

a)	ACC_raw	p-value
FD ML	–	–

b)	ACC_raw	p-value	ACC_2f95	p-value	ACC_f95	p-value	ACC_3.5	p-value	ACC_0.5	p-value
PATH	–	–	0.18 [0.03:0.33]	1.8E-02	**0.42 [0.29:0.54]**	1.3E-08	**0.51 [0.38:0.62]**	2.8E-12	**0.62 [0.50:0.71]**	3.1E-19
PATH AP	–	–	0.14 [-0.02:0.29]	6.9E-02	0.31 [0.16:0.44]	5.1E-05	**0.41 [0.27:0.54]**	2.7E-08	**0.54 [0.41:0.65]**	2.8E-14
PATH ML	–	–	0.17 [0.02:0.31]	2.5E-02	0.36 [0.21:0.49]	2.3E-06	**0.44 [0.30:0.56]**	3.6E-09	**0.62 [0.52:0.71]**	3.3E-19
DIST	0.40 [0.26:0.53]	7.8E-08	**0.44 [0.31:0.56]**	3.2E-09	**0.44 [0.31:0.57]**	1.8E-09	**0.44 [0.31:0.56]**	1.6E-09	**0.38 [0.24:0.51]**	3.4E-07
DIST AP	0.30 [0.16:0.43]	6.2E-05	0.33 [0.18:0.46]	1.3E-05	0.33 [0.20:0.46]	9.5E-06	0.33 [0.19:0.47]	9.8E-06	0.29 [0.14:0.42]	1.4E-04
DIST ML	**0.50 [0.37:0.60]**	6.7E-12	**0.53 [0.42:0.63]**	1.5E-13	**0.54 [0.43:0.65]**	2.9E-14	**0.55 [0.44:0.64]**	8.9E-15	**0.57 [0.45:0.68]**	3.7E-16
RMS	0.39 [0.25:0.52]	1.5E-07	**0.42 [0.29:0.54]**	1.2E-08	**0.43 [0.29:0.55]**	5.9E-09	**0.43 [0.30:0.55]**	4.2E-09	0.37 [0.23:0.50]	9.4E-07
RMS AP	0.31 [0.17:0.44]	5.3E-05	0.34 [0.19:0.47]	8.0E-06	0.34 [0.19:0.47]	9.0E-06	0.34 [0.19:0.46]	8.2E-06	0.30 [0.16:0.43]	9.6E-05
RMS ML	**0.52 [0.40:0.62]**	6.9E-13	**0.55 [0.44:0.64]**	1.1E-14	**0.56 [0.45:0.65]**	2.2E-15	**0.57 [0.46:0.67]**	3.9E-16	**0.60 [0.48:0.69]**	1.6E-17
RANGE	0.38 [0.23:0.50]	5.4E-07	0.35 [0.21:0.47]	4.2E-06	0.39 [0.26:0.51]	1.4E-07	**0.41 [0.28:0.52]**	4.4E-08	**0.42 [0.29:0.55]**	1.3E-08
RANGE AP	0.24 [0.10:0.38]	1.7E-03	0.20 [0.05:0.34]	1.1E-02	0.26 [0.12:0.39]	7.6E-04	0.28 [0.14:0.41]	2.8E-04	0.32 [0.18:0.46]	1.8E-05
RANGE ML	**0.51 [0.38:0.62]**	1.8E-12	**0.53 [0.40:0.63]**	1.5E-13	**0.55 [0.43:0.65]**	1.2E-14	**0.58 [0.46:0.68]**	2.8E-16	**0.61 [0.51:0.71]**	3.2E-18
MV	–	–	0.18 [0.03:0.32]	1.8E-02	**0.42 [0.29:0.54]**	1.3E-08	**0.51 [0.37:0.62]**	2.8E-12	**0.62 [0.51:0.71]**	3.1E-19

(*continued on next page*)

Table 3 (*continued*)

MV AP	–	–	0.14 [-0.01:0.29]	6.9E-02	0.31 [0.15:0.43]	5.1E-05	**0.41 [0.26:0.53]**	2.7E-08	**0.54 [0.41:0.65]**	2.8E-14
MV ML	–	–	0.17 [0.02:0.33]	2.5E-02	0.36 [0.21:0.48]	2.3E-06	**0.44 [0.30:0.56]**	3.6E-09	**0.62 [0.51:0.71]**	3.3E-19
AREA	0.37 [0.22:0.48]	1.1E-06	**0.51 [0.40:0.62]**	1.2E-12	**0.55 [0.44:0.65]**	1.4E-14	**0.57 [0.45:0.66]**	1.4E-15	**0.58 [0.47:0.68]**	1.7E-16
MF	–	–	–	–	–	–	–	–	–	–

Qualitatively, there was no consensus on which foam surface was the most challenging, with 8 participants selecting FF, 7 selecting SF, and 6 selecting MF.

3.5. *Effect of visual condition*

Refer to Table S1 for detailed numerical data.

3.5.1. *Frequency domain parameters*

GRF-based PWR and PWR AP increased significantly in EC. No other significant difference was found for the other frequency domain metrics either GRF- or IMU-based.

3.5.2. *Time domain parameters*

GRF-based PATH and MV, in AP direction or in module, and AREA were higher in EC condition regardless of the surface. Also, GRF-based RANGE and RANGE AP were higher in the EC condition on all surfaces, but this difference was significant only when participants were standing on foam.

For IMU-based metrics, the only significant differences were found on DIST ML and RMS ML for ACC_f95, ACC_3.5, and ACC_0.5 that decreased in EC when standing on a foam.

Exemplificative results are shown in Fig. 3 for AREA, MV, and RMS ML.

4. Discussion

The quantitative analysis of posture by means of metrics computed from GRF data has become a reference for the investigation of postural performance during standing and of the physiological mechanisms underlying postural control, in particular, for multisensory integration (Paillard and Noé, 2015). In recent years, due to their ease of use and portability, IMUs have been proposed as an alternative to force platform for postural assessment, but, although their recognised potential in identifying postural alterations, still, functional interpretation of IMU-based postural metrics is critical, and understanding of the influence of testing and processing procedures, filtering in particular, is lacking.

This study compared GRF- and IMU-based posture metrics in healthy adults for changing visual and surface conditions, concurrently analysing how results are affected by filtering of trunk ACC (approximating CoM-ACC), aiming to provide a better understanding of functional interpretation of IMU-based metrics and their sensitivity to operative conditions.

In the literature, low-pass filtering used for IMU-based metrics calculation ranges from 0.5 Hz to no filtering at all (Dalton et al., 2013; Ghislieri et al., 2019). As related to the power content of the raw IMU-based postural signal, Reynard et al. (Reynard et al., 2019) found F95 up to 15 Hz, using a sensor attached to the chest during a variety of postural tasks, including standing on one leg and standing on a rocking board. In the present study, analysing lumbar sensor placement during standard standing posture, power analysis of ACC_raw showed maximum values of 4.9 Hz for F95, of 4.2 Hz for F80, and of 2.6 Hz for F50, while F95 of GRF-based signal always remained below 2.1 Hz, implying that standard 10 Hz low-pass filtering of GRF signals does not produce any relevant loss of information. These results indicate that filtering IMU-based postural signal below 5 Hz (approximating to integer 4.9 Hz) will produce a significant loss in power, thus, potentially implying a significant loss in the informative content of the acceleration signal itself. On the other hand, the general requirement of a certain degree of filtering when the sampling frequency is much higher than signal maximal frequency, as in this study, is supported by the poor correlation (see Table 2) between GRF- and IMU-based metrics for ACC_raw and ACC_2f95 (cut-off frequency 10 Hz), that increase in number of parameters and quality for ACC_3.5 and ACC_0.5.

Nevertheless, correlation between GRF- and IMU-based metrics never resulted more than moderate for 8 out of 17 time-based

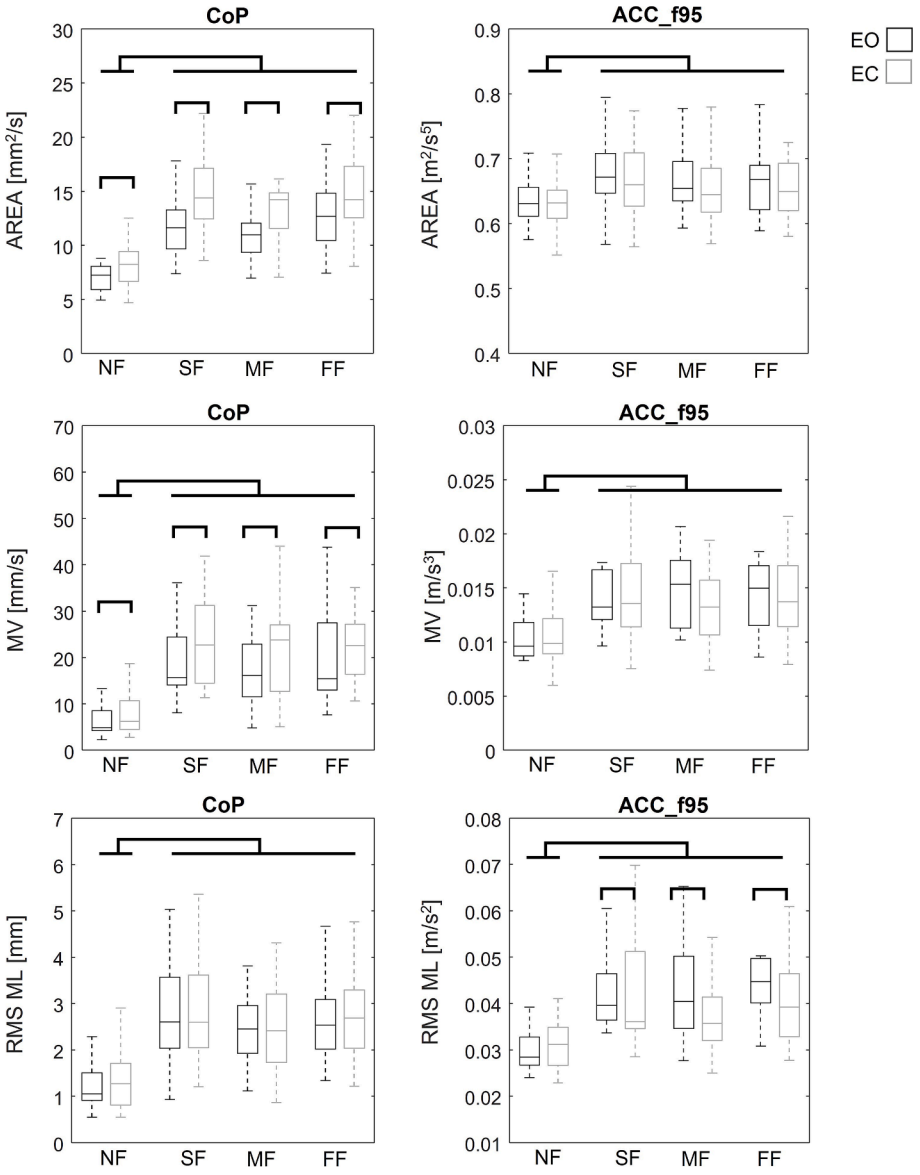

Fig. 3. a) GRF-based and b) IMU-based AREA, MV, and RMS ML in the different conditions (no foam, NF, soft foam, SF, medium foam, MF, firm foam, FF, eyes open, EO (in black), eyes closed, EC (in grey)).

parameters for ACC_f95 (cut-off frequency 5 Hz) (i.e., when all the informative content of IMU-based signal is included in the analysis), and for 13 and for 11 out of 17 for ACC_3.5 and ACC_0.5 respectively, with slightly higher ρ values for the latter. These results seem to support the hypothesis that, although describing the same behavior (i.e. postural control), GRF- and IMU-based metrics target different specific manifestations of postural control that, according to the inverse pendulum approximation (Gage et al., 2004; Winter, 1995) can be described as: i) the trajectory of CoP for GRF-based metrics; ii) the CoM-CoP distance (proportional to CoM-ACC) for IMU-based metrics.

When examining the effects of surface and visual conditions, generally, both GRF- and IMU-based metrics resulted to be significantly affected by foam and EC. Nevertheless, how these operative conditions affected metrics calculated in the time and frequency domain differed for GRF- and IMU-based ones.

Considering frequency metrics, for instance, only GRF-based PWR, PWR AP, CF, and CF AP showed a significant change, specifically an increase for all, when standing on foam, independently on the type of foam, while among IMU-based metrics, similarly, PWR and PWR AP showed a significant increase, but F50 and CF decreased in both AP and ML directions. This relevant difference highlights the change in target of the metrics calculated on different signals: when standing on foam, the oscillation of the CoP increases both in amplitude and frequency power distribution over the same range in the AP direction, while the oscillation of the CoM-CoP distance (related to CoM-ACC) increases in amplitude in the AP direction, while becoming slower in both AP and ML directions. This interpretation is supported also by the results in the time domain, where both GRF- and IMU-based metrics increase, except for MF, non-changing for GRF-based and decreasing for IMU-based; PATH and MV showing no foam effect only for Acc_raw and Acc_2f95, possibly due to lower signal to noise ratio.

The absence of significant differences in post-hoc analysis among different foam surfaces, similarly to previous research (Patel et al., 2008), suggests that, although differences in stiffness are perceived subjectively, once a certain level of surface instability is introduced, further changes in foam stiffness do not proportionally affect postural control (i.e. CoP sway and associated CoM-CoP distance dynamics) in young healthy subjects.

When analysing EO versus EC conditions, CoP-based PATH, MV, RANGE, calculated bi-dimensionally and on the AP axis, and AREA

increased in EC condition, particularly on foam surfaces, as expected (Huang et al., 2022). Conversely, ACC-based metrics did not show significant differences between the two visual conditions, except for DIST ML and RMS ML that decreased in the EC condition when participants stood on foam. Here again, the change in motor strategy (i.e. CoP dynamics) for the maintenance of balance is described by GRF-based metrics, while IMU-based ones describe the resulting control action as CoM-CoP dynamics, being CoM-CoP distance the error signal within the postural control system (Noamani et al., 2023; Winter, 1995).

By interpreting results from this perspective, the foam surface results to impact both motor performance (i.e. GRF-based metrics) and control system performance (i.e. IMU-based metrics), but in different ways (i.e. increase in amplitude for both, but decrease in frequency for the latter): in young healthy adults, the lack of visual input leads to postural performance adjustments, as shown by increased GRF-based metrics, efficiently preserving control system performance (i.e. unvaried IMU-based metrics) in terms of CoM-CoP distance maintenance in AP direction, and reduction in ML one (i.e. IMU-based DIST and RMS) under EC + foam condition.

Present results highlight how both GRF- and IMU-based metrics can serve as descriptors of postural control, but rather than being alternative, they can be considered complementary measures, in the analysed operative conditions (i.e. comfortable standing posture with the feet under the hips, subjects that exhibit an ankle strategy): GRF-based ones describing the integral effect of the motor strategy implemented by postural control; IMU-based ones the resulting control performance (Noamani et al., 2023; Winter, 1995). This interpretation cannot be generalised to different postural assessment conditions, such as tandem and/or standing on one foot, where a CoM control strategy can come into play, and for which further analysis is required (Morasso, 2020).

From a methodological point of view, future studies must aim to standardise IMU-signal filtering to support proper interpretation and allow comparability and integration of future results. Based on the present findings, when analysing young healthy adults in static posture with IMU-sensor at lumbar level, a 5 Hz cut-off frequency resulted to allow noise reduction maintaining 95 % of the power of the signal.

In conclusion, although limited to the analysis of postural control in a population of young healthy adults for varying surface and visual conditions, this study highlighted the importance of the filtering of IMU-based signals for the proper interpretation of the resulting postural metrics, and the potential of GRF- and IMU-based metrics integration for a better understanding of postural control. Future works should analyse different populations (e.g., elderly, pathologic), and/or postural tasks and testing conditions to identify differences in postural adjustments and control performance, after performing a frequency analysis of the IMU-signal to determine the appropriate cut-off frequency for filtering.

Declaration of competing interest

The authors declare that they have no known competing financial interests or personal relationships that could have appeared to influence the work reported in this paper.

Appendix

Description of time domain metrics calculation (Mancini et al., 2012; Prieto et al., 1996).

First, the target signal (ACC or CoP) components along AP and ML were detrended (Xd) by subtracting the trial-specific mean ($\overline{X}$):

$$Xd_i = X_i - \overline{X}$$

where i represents the i-th frame.

The following description is provided for a general signal vector X (either CoP or ACC, component or vector's magnitude). The specific components on which the metrics were calculated are described in Table 2.

- DIST: Mean distance from the centre of signal trajectory.

$$DIST = \frac{1}{nf}\sum_{i=1}^{nf}(Xd_i)$$

Where nf represents the number of frames.

- RMS: Root mean square of signal time series

$$RMS = \mathrm{rms}(Xd)$$

- PATH: Sway path, total length of signal trajectory

$$PATH = \sum_{i=1}^{nf-1}|Xd_{i+1} - Xd_i|$$

- RANGE: Range of displacement

$$RANGE = \max(Xd) - \min(Xd)$$

- MV: Mean Velocity

$$MV = \frac{PATH}{trial\ duration}$$

- MF: Mean frequency, the number, per second, of loops that have to be run by *X (module)*, to cover a total trajectory equal to *PATH*

$$MF = \frac{PATH}{2*\pi*DIST*trial\ duration}$$

- Area: area spanned by *X (*module) per unit of time

$$AREA = \frac{\sum_{i=1}^{nf-1} |Xd\_ap_{i+1}*Xd\_ml_i - Xd\_ap_i*Xd\_ml_{i+1}|}{2*trial\ duration}$$

Where *Xd_ap* and *Xd_ml* represent the detrended signal components along AP and ML direction, respectively.

Appendix A. Supplementary data

Supplementary data to this article can be found online at https://doi.org/10.1016/j.jbiomech.2025.112687.

References

Dalton, A., Khalil, H., Busse, M., Rosser, A., van Deursen, R., ÓLaighin, G., 2013. Analysis of gait and balance through a single triaxial accelerometer in presymptomatic and symptomatic Huntington's disease. Gait Posture 37, 49–54. https://doi.org/10.1016/j.gaitpost.2012.05.028.

Gage, W.H., Winter, D.A., Frank, J.S., Adkin, A.L., 2004. Kinematic and kinetic validity of the inverted pendulum model in quiet standing. Gait Posture 19, 124–132. https://doi.org/10.1016/S0966-6362(03)00037-7.

Gera, G., Chesnutt, J., Mancini, M., Horak, F.B., King, L.A., 2018. Inertial sensor-based assessment of central sensory integration for balance after mild traumatic brain injury. Mil. Med. 183, 327–332. https://doi.org/10.1093/milmed/usx162.

Ghislieri, M., Gastaldi, L., Pastorelli, S., Tadano, S., Agostini, V., 2019. Wearable inertial sensors to assess standing balance: A systematic review. Sensors 19, 4075. https://doi.org/10.3390/s19194075.

Y. Hochberg, A.C. Tamhane, 2008. References, in: Multiple Comparison Procedures. John Wiley & Sons, Inc., pp. 417–438.

Huang, C.-C., Jaw, F.-S., Young, Y.-H., 2022. Radiological and functional assessment in patients with lumbar spinal stenosis. BMC Musculoskelet. Disord. 23, 137. https://doi.org/10.1186/s12891-022-05053-x.

Huisinga, J., Mancini, M., Veys, C., Spain, R., Horak, F., 2018. Coherence analysis of trunk and leg acceleration reveals altered postural sway strategy during standing in persons with multiple sclerosis. Hum. Mov. Sci. 58, 330–336. https://doi.org/10.1016/j.humov.2017.12.009.

Mancini, M., Salarian, A., Carlson-Kuhta, P., Zampieri, C., King, L., Chiari, L., Horak, F. B., 2012. ISway: a sensitive, valid and reliable measure of postural control. J. Neuroengineering Rehabil. 9, 59. https://doi.org/10.1186/1743-0003-9-59.

McIlroy, W.E., Maki, B.E., 1997. Preferred placement of the feet during quiet stance: development of a standardized foot placement for balance testing. Clin. Biomech. Bristol Avon 12, 66–70. https://doi.org/10.1016/s0268-0033(96)00040-x.

Miller, E.J., Sheehan, R.C., Kaufman, K.R., 2022. IMU filter settings for high intensity activities. Gait Posture 91, 26–29. https://doi.org/10.1016/j.gaitpost.2021.10.006.

Morasso, P., 2020. Centre of pressure versus centre of mass stabilization strategies: the tightrope balancing case. R. Soc. Open Sci. 7, 200111. https://doi.org/10.1098/rsos.200111.

Noamani, A., Riahi, N., Vette, A.H., Rouhani, H., 2023. Clinical static balance assessment: A narrative review of traditional and IMU-based posturography in older adults and individuals with incomplete spinal cord injury. Sensors 23, 8881. https://doi.org/10.3390/s23218881.

Paillard, T., Noé, F., 2015. Techniques and methods for testing the postural function in healthy and pathological subjects. Biomed Res. Int. 2015, 891390. https://doi.org/10.1155/2015/891390.

Palmerini, L., Rocchi, L., Mellone, S., Valzania, F., Chiari, L., 2011. Feature selection for accelerometer-based posture analysis in Parkinson's disease. IEEE Trans. Inf Technol. Biomed. 15, 481–490. https://doi.org/10.1109/TITB.2011.2107916.

Patel, M., Fransson, P.A., Lush, D., Gomez, S., 2008. The effect of foam surface properties on postural stability assessment while standing. Gait Posture 28, 649–656. https://doi.org/10.1016/j.gaitpost.2008.04.018.

R.J. Peterka, 2018. Chapter 2 - Sensory integration for human balance control, in: Day, B. L., Lord, S.R. (Eds.), Handbook of Clinical Neurology, Balance, Gait, and Falls. Elsevier, pp. 27–42. https://doi.org/10.1016/B978-0-444-63916-5.00002-1.

Pirini, M., Bisi, M.C., Turolla, A., Agostini, M., Vidale, D., Fiorentin, A., Piron, F., 2018. Postural rehabilitation within the VRRS (virtual reality rehabilitation system) environment. Adv. Technol. Rehabil. Gait Balance Disord. 335–355. https://doi.org/10.1007/978-3-319-72736-3_24.

Prieto 1, Myklebust, J.B., Hoffmann, R.G., Lovett, E.G., Myklebust, B.M., 1996 Sep. Measures of postural steadiness: differences between healthy young and elderly adultsT E. IEEE Trans Biomed Eng. 43 (9), 956–966. https://doi.org/10.1109/10.532130.

Quijoux, F., Nicolaï, A., Chairi, I., Bargiotas, I., Ricard, D., Yelnik, A., Oudre, L., Bertin-Hugault, F., Vidal, P.-P., Vayatis, N., Buffat, S., Audiffren, J., 2021. A review of center of pressure (COP) variables to quantify standing balance in elderly people: Algorithms and open-access code*. Physiol. Rep. 9, e15067. https://doi.org/10.14814/phy2.15067.

Reynard, F., Christe, D., Terrier, P., 2019. Postural control in healthy adults: Determinants of trunk sway assessed with a chest-worn accelerometer in 12 quiet standing tasks. PLoS One 14, e0211051. https://doi.org/10.1371/journal.pone.0211051.

Schober, P., Boer, C., Schwarte, L.A., 2018. Correlation coefficients: Appropriate use and interpretation. Anesth. Analg. 126, 1763. https://doi.org/10.1213/ANE.0000000000002864.

Winter, D., 1995. Human balance and posture control during standing and walking. Gait Posture 3, 193–214. https://doi.org/10.1016/0966-6362(96)82849-9.